A NEW CONCEPT IN INCREASING STABILITY OF METAL STRUCTURES UNDER PRESTRESS

Thesis for the Degree of M. S.
MICHIGAN STATE UNIVERSITY
A. G. Patwardhan
1963

A NEW CONCEPT IN INCREASING STABILITY OF METAL STRUCTURES UNDER PRESTRESS

By

A. G. Patwardhan

A THESIS

Submitted to
Michigan State University
in partial fulfillment of the requirements
for the degree of

MASTER OF SCIENCE

Department of Civil Engineering

1963

ACKNOWLEDGMENT

I wish to record my sincere thanks to Dr. C. E. Cutts, Dr. R. K. Wen, Dr. W. A. Bradley and Dr. J. L. Lubkin for their very valuable guidance and all the help given to me in preparation of this thesis.

Mr. Don Childs and the staff of the Division of Engineering Research did some excellent work in preparation of the experimental models. Their help is gratefully acknowledged.

****

TABLE OF CONTENTS

SYNOPSIS

This paper concerns itself mainly with the stability of a metal structural member under prestress. A very simple method to increase the stability under high compressive prestressing loads has been discussed and a mathematical analysis based on linear elastic and small deflection theory has been worked out. Results of experiments on an aluminum and a steel model are given in Part II of the paper. Part III is devoted to a few examples of practical applications, illustrating the economy in materials and fabrication costs.

It is shown that by maintaining the prestressing forces on both sides of the member under prestress, at fixed equal distances from the center line of the member, and at a number of points in the span, the buckling strength of the member can be increased many-fold. This fact is also demonstrated experimentally.

I. INTRODUCTION

During the last twenty years, great strides have been made in the use of prestressed concrete. The low tensile strength of concrete has been offset by inducing high compressive stresses in regions, where,under service loads, tensile stresses would develop. An extension of this idea to metal structures is a natural corollary and several excellent papers on this subject have already been published (references 1, 3, 4, 5 and 6 of bibliography). Starting with simple units such as a member carrying a direct tensile force these papers illustrate how the prestressing technique can be effectively employed for more complex structures. Prestressed steel construction has not been widely adopted, mainly because of the instability of relatively thin sections under high prestressing forces. Some of the other reasons are the availability of high strength steels in the form of usual structural sections, the difficulty in protecting steel prestressing cables from the elements and the high cost of prestressing at the site of construction.

The problem of instability is not a consideration in prestressed concrete construction, where the prestressing elements are embedded throughout their lengths within the section itself and are symmetrically located about the weaker axis of bending. In the case of metal structures, however, the cables must be placed outside the section and the buckling of the member becomes one of primary concern.

The method to improve stability proposed in this paper is both simple and effective. The equal prestressing forces on the two sides of the member are maintained at fixed equal distances from the axis about which buckling would occur. This is accomplished by passing the cables through spacers fixed to the member at a number of points throughout the

span. By this means, considerable resistance to buckling is obtained. With the buckling of the member, the prestressing wires must follow the bent form at all points where they pass through spacers fixed to the member. In this deformed state, the tensions in the wires on both the sides of any spacer and on both the sides of the member have lateral components of the same sign. These lateral loads produce a bending moment in the member which tends to straighten the bent form. This stabilizing effect is in addition to that provided by the internal bending stresses produced in the member. The closer the spacing of the spacers, the greater is the stability of the member. A minimum distance between the spacers can be found so that a given axial prestressing force does not cause instability in the member being prestressed. This is the problem which is considered in detail in the following paragraphs.

Buckling Load Under Prestress

Notation:

L = Total length of the member.

ℓ = Length between adjacent spacers (assumed equal).

n = Number of equal panels, $L = n\ell$.

A = Area of prestressing wires on one side.

E = Modulus of elasticity of the wires.

E_b = Modulus of elasticity of the member.

I_b = Moment of inertia of the member about the axis about which buckling occurs.

T = Tensile force in the wires on one side of the member.

T_o = Tensile force in the wires on one side at buckling.

δT, δT_o = Change in tension in the wires on one side as a result of bending of the member.

d = Distance from the center line of the wires to the longitudinal axis of the member, at the points where the wires pass through spacers.

y_x = Deflection of any point from the original straight axis.

y_k = Deflection of the point at the k^{th} spacer.

y'_x , y''_x = First and second derivatives of y with respect to x.

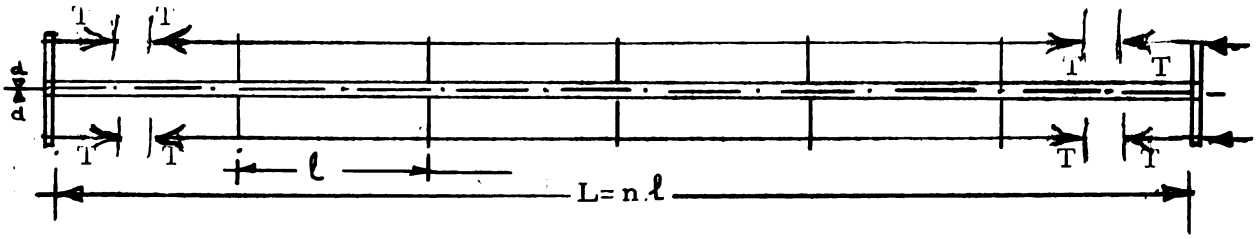

Figure 1

Figure 1 shows the member under the action of prestressing tensions T, symmetrical about the longitudinal axis of the member. At some tension T_o, the member will be in a state of neutral equilibrium, when both the straight and the bent configurations are static. The straight form constitutes the trivial solution. An equation of the elastic curve in the buckled state, which satisfies the conditions of equilibrium and continuity must then be found. Figure 2 shows the member in this latter state when the prestressing tension is at its critical value.

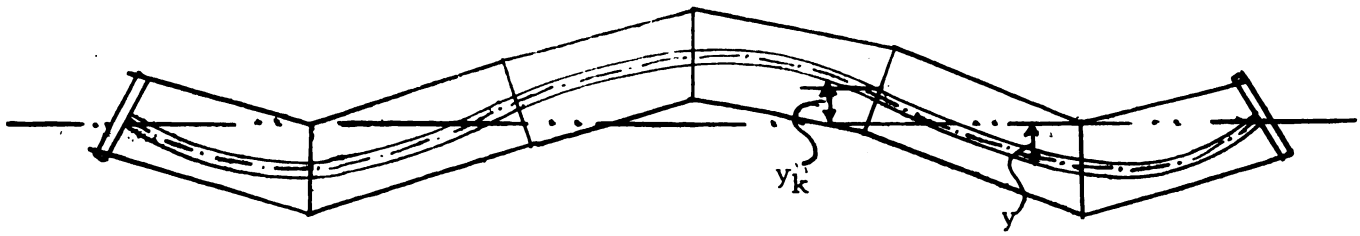

Figure 2

In the following derivation axial shortening of the member is neglected and where terms such as ℓ and L occur in the derivation, the effect of axial shortening is considered negligible.

The tensions in the wires on the two sides of the member will undergo changes as a result of bending of the member. The changes will depend on the changes in the original lengths of the wires on the two sides.

Consider one of the segments of the member between the $(k-1)^{th}$ and the k^{th} spacer (Figure 3). In this segment, the shortening of the wire on the concave side of the curve is $\delta\ell = d\{\sin(y'_{k-1}) - \sin(y'_k)\}$ see θ_k

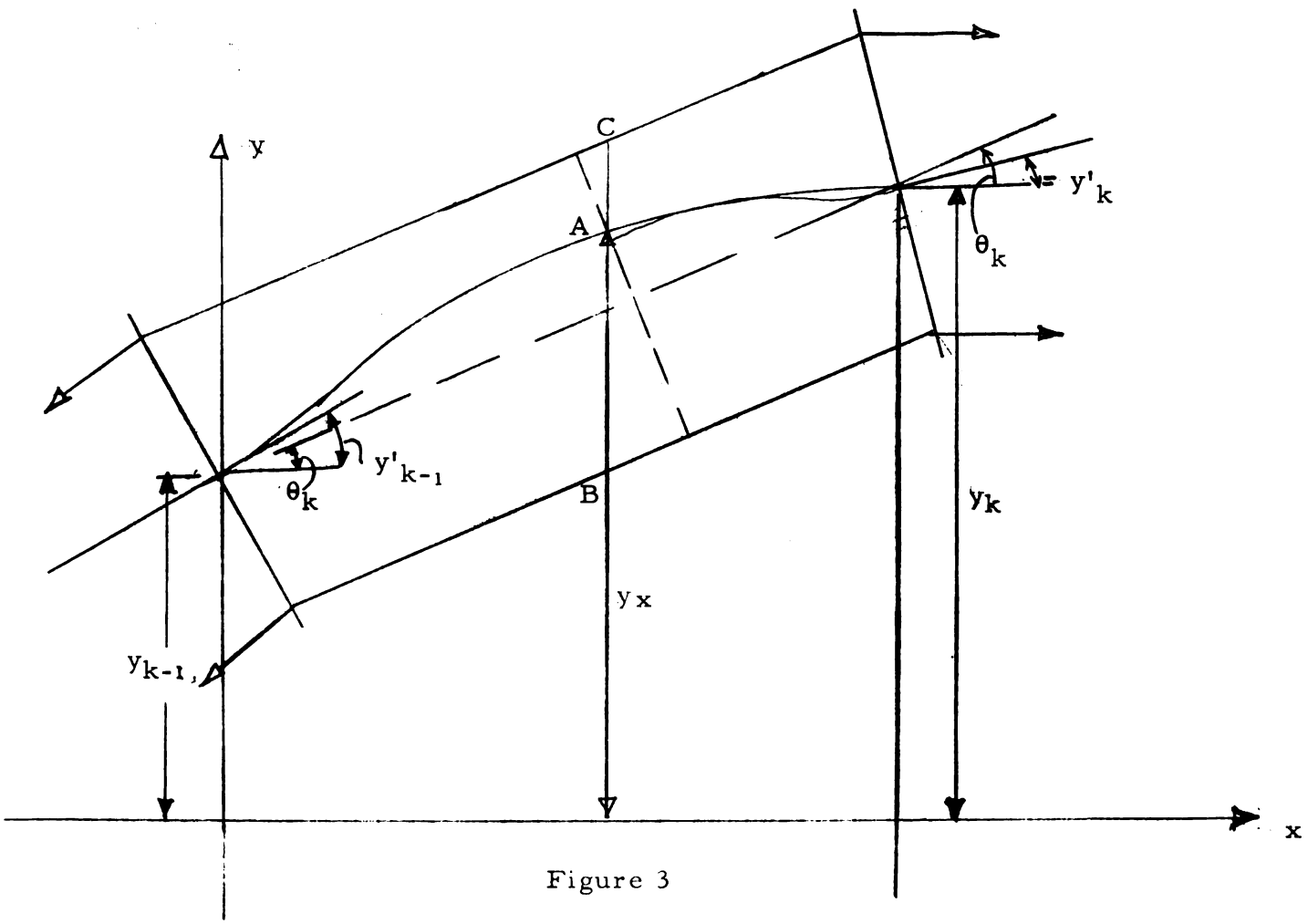

Figure 3

For small deflections and consequently small angles, sine of the angle = tangent of the angle = the angle in radians and sec $\theta_k \simeq 1$,

$$\therefore \quad \delta \ell = d\,(y'_{k-1} - y'_k) \quad \ldots\ldots\ldots \text{(a)}$$

$$\text{Total change in length} = \delta L = d \sum_{k=1}^{n} (y'_{k-1} - y'_k) \quad \ldots\ldots \text{(b)}$$

$$\text{but} \sum_{k=1}^{n} (y'_{k-1} - y'_k) = y'_o - y'_n$$

$$\therefore \quad \delta L = d(y'_o - y'_n) \quad \ldots\ldots\ldots\ldots \text{(1)}$$

$$\text{The change in tension} = \delta T_o = \frac{A\,E\,\delta\,L}{L} =$$

$$\therefore \quad \delta T_o = \frac{A\,E\,d}{L}(y'_o - y'_n) \quad \ldots\ldots\ldots \text{(2)}$$

The sign of $\delta\ T_o$ will depend on the sign of the term $(y'_o - y'_n)$.

By similar reasoning, the change in tension in the wires on the other side will be of the same magnitude, but opposite in sign.

It will now be shown, that neglecting friction, the tensions in the wires on both the sides of any spacer have equal magnitudes for small deflection of the member.

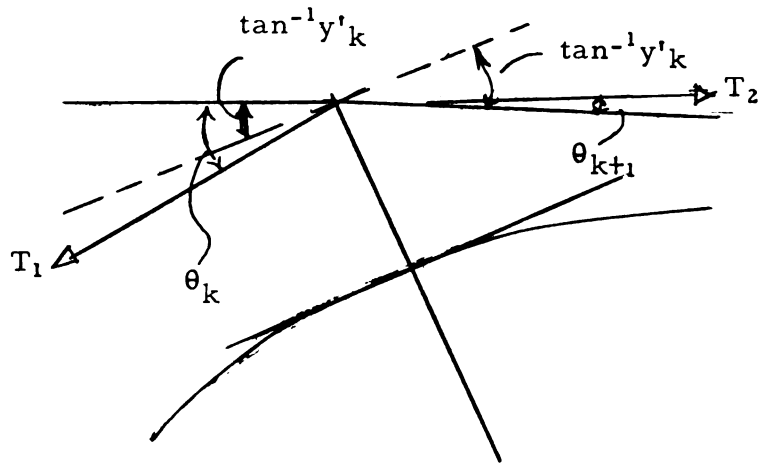

Figure 4

Referring to Figure 4, the components of tensions at right angles to any spacer must balance.

If T_2 and T_1 are the tensions on the two sides of any spacer, then,

$$T_2 \cos (y'_k - \theta_{k+1}) = T_1 \cos (\theta_k - y'_k)$$

Since y'_k, θ_k and θ_{k+1} are all small angles,

$$T_2 \simeq T_1.$$

Thus in the buckled state, the tension in the wires on one side will be $T_o + \delta T_o$ while that in the wires on the opposite side of the member will be $T_o - \delta T_o$. The tensions in the wires on any side will, for all practical purposes, be uniform throughout their lengths.

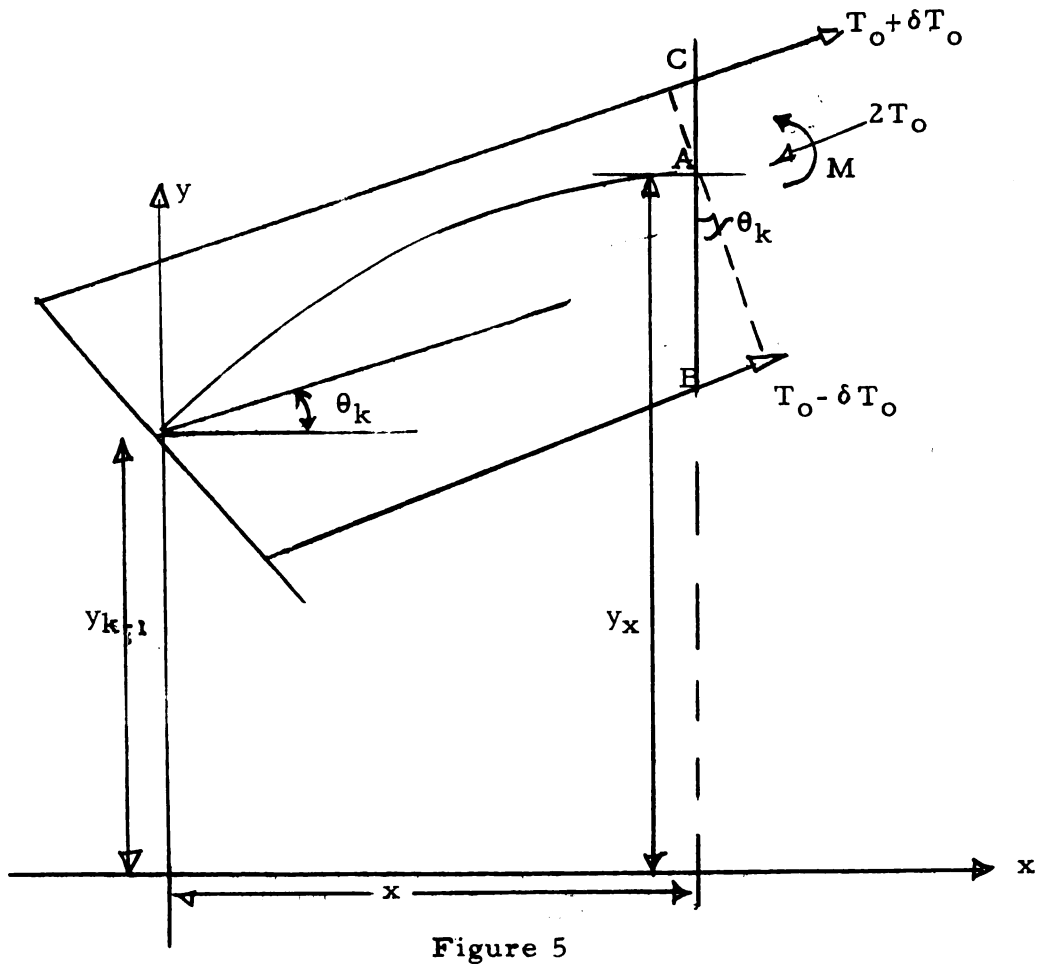

Figure 5

Figure 5 shows the free body diagram of the segment, obtained after making a cut at any point between the $(k-1)^{th}$ and the k^{th} spacers. All other forces are self equilibrated and the only external forces acting on the member are $T_o + \delta T_o$ and $T_o - \delta T_o$.

The axes chosen are shown in the figure. Bending moment at any point distant x from the $(k-1)^{th}$ spacer is

$$M_x = (T_o - \delta T_o)\, AB \cos\theta_k - (T_o + \delta T_o)\, AC \cos\theta_k$$

Again assuming $\cos\theta_k \simeq 1$

$$M_x = (T_o - \delta T_o)\, AB - (T_o + \delta T_o)\, AC \quad \ldots\ldots\ldots \text{(c)}$$

$$AB = y_x - \left\{ y_{k-1} - d + (y_k - y_{k-1}) \frac{x}{\ell} \right\} \quad \ldots\ldots\ldots \text{(d)}$$

$$AC = \left\{ y_{k-1} + d + (y_k - y_{k-1}) \frac{x}{\ell} \right\} - y_x \quad \ldots\ldots\ldots \text{(e)}$$

$$\delta T_o = \frac{A E d}{L} (y'_o - y'_n) \quad \ldots\ldots\ldots\ldots\ldots\ldots \text{(2)}$$

$$\therefore\ M_x = \left[T_o - \frac{A E d}{L} (y'_o - y'_n)\right] \left[y_x - \left\{ y_{k-1} - d + (y_k - y_{k-1}) \frac{x}{\ell} \right\} \right]$$

$$- \left[T_o + \frac{A E d}{L} (y'_o - y'_n)\right] \left[\left\{ y_{k-1} + d + (y_k - y_{k-1}) \frac{x}{\ell} \right\} - y_x \right]$$

which upon simplifying gives,

$$M_x = 2T_o \left\{ y_x - y_{k-1} - (y_k - y_{k-1}) \frac{x}{\ell} \right\} - \frac{2d^2 AE}{L} (y'_o - y'_n) \quad \ldots \text{(f)}$$

but $M_x = -E_b I_b\, y''_x$

$$\therefore\ -E_b I_b\, y''_x = 2T_o \left\{ y_x - y_{k-1} - (y_k - y_{k-1}) \frac{x}{\ell} \right\} - \frac{2d^2 AE}{L} (y'_o - y'_n)$$

$$\therefore\ y''_x + \frac{2T_o}{E_b I_b} y_x = \frac{2T_o}{E_b I_b} \left\{ y_{k-1} + (y_k - y_{k-1}) \frac{x}{\ell} \right\} + \frac{2d^2 AE}{E_b I_b L} (y'_o - y'_n) \quad \ldots \text{(3)}$$

Setting $\frac{2T_o}{E_b I_b} = p^2$ leads to the standard form of a second order linear differential equation,

$$y''_x + p^2 y_x = p^2 \left\{ y_{k-1} + (y_k - y_{k-1}) \frac{x}{\ell} \right\} + p^2 \frac{d^2 AE}{T_o L} (y'_o - y'_n) \quad \ldots \text{(4)}$$

Solution of this equation is

$$y_x = C_1 \cos px + C_2 \sin px + \left\{ y_{k-1} + (y_k - y_{k-1}) \frac{x}{\ell} \right\} + \frac{d^2 AE}{T_o L} (y'_o - y'_n) \quad . . \quad (5)$$

The constants C_1 and C_2 are the two constants which must be determined from the boundary conditions. Setting $x = 0$ in equation (5)

$$y_{k-1} = C_1 + \frac{d^2 AE}{T_o L} (y'_o - y_n) + y_{k-1} \quad \text{from which,}$$

$$C_1 = - \frac{d^2 AE}{T_o L} (y'_o - y'_n) \quad . . . . \quad (g)$$

Setting $x = \ell$ in equation (5),

$$y_k = C_1(\cos p\ell - 1) + y_k + C_2 \sin p\ell \quad \text{from which,}$$

$$C_2 = C_1 \frac{(1 - \cos p\ell)}{\sin p\ell} \quad . . . . . \quad (h)$$

Thus the equation of the deflected curve of any segment is;

$$y_x = C_1 (\cos px - 1) + C_1 \frac{(1 - \cos p\ell)}{\sin p\ell} + y_{k-1} + (y_k - y_{k-1}) \frac{x}{\ell} \quad . . . \quad (6)$$

If $C_1 \neq 0$, the deflection will be indefinitely large for $\sin p\ell = 0$ or $p\ell = n\pi$ where n is odd. For even values of n the second term becomes indeterminate. Differentiating (5) with respect to x

$$y'_x = - C_1 p \sin px + C_2 p \cos px + \frac{(y_k - y_{k-1})}{\ell} \quad . . . . \quad (i)$$

Substituting $x = 0$ in the above equation

$$y'_{k-1} = C_2 p + \frac{(y_k - y_{k-1})}{\ell} \quad . . . . \quad (j)$$

and substituting $x = \ell$ in equation (i)

$$y'_k = -C_1 p \sin p\ell + C_2 p \cos p\ell + \frac{(y_k - y_{k-1})}{\ell} \quad . . . \quad (k)$$

Subtracting (k) from (j)

$$y'_{k-1} - y'_k = C_1 p \sin p\ell + C_2 p (1 - \cos p\ell) . . . . . \quad (l)$$

and summing over the 'n' panels

$$\sum_{k=1}^{n} y'_{k-1} - y'_k = y'_o - y'_n = p \sin p\ell \sum C_1 + p(1-\cos p\ell) \sum C_2 \quad \ldots \quad (m)$$

where ΣC_1 and ΣC_2 represent the sums of the two constants obtained for each of the n panels.

For the case when $C_1 \neq 0$ C_1 is independent of any properties peculiar to any segment and hence is the same for all the segments. So is C_2 because $C_2 = C_1 \frac{(1-\cos p\ell)}{\sin p\ell}$. We have also seen that in this case, the lowest buckling load is that given by $p\ell = \pi$.

If $C_1 = 0$, then C_2 is indeterminate if $p\ell = \pi$

Also since $C_1 = \frac{d^2AE}{T_oL}$ $(y'_o - y'_n)$, the last term in the parenthesis must be zero, i.e., $y'_o - y'_n = 0$

The equation of the deflected form is, in this case,

$$y_x = C_2 \sin px + y_{k-1} + (y_k - y_{k-1}) \frac{x}{\ell} \quad \ldots \quad (n)$$

and setting $x = \ell$ in equation (n)

$$y_k = C_2 \sin p\ell + y_k \text{ or } C_2 \sin p\ell = 0 \quad \ldots \quad (7)$$

Now if $C_1 = 0$, C_2 cannot be zero for a nontrivial solution. $\therefore \sin p\ell = 0$ or $p\ell = n\pi$

The lowest buckling load is again, therefore, given by

$$p\ell = \pi \quad \text{or} \quad 2T_o = \frac{\pi^2 E_b I_b}{\ell^2} \quad \ldots \quad (8)$$

Referring again to equation (6), we find that for $\sin p\ell = 0$, y_x becomes infinite if C_1 is not zero. Since this is impossible, sin pl = 0 necessarily implies that $C_1 = 0$ because only in that case, can C_2 have an indeterminate value. We thus arrive at the condition that in the buckled state $y'_o - y'_n = 0$ . . . . (A).

From equation (m) we have,

$y'_o - y'_n = 0 = p(1-\cos p\ell) \sum C_2$ and since $(1 - \cos p\ell)$ is not zero for $p\ell = \pi$, $\Sigma C_2 = 0$ . . . . . (B)

Thus we arrive at two important conditions governing the buckled configuration of the member. They are: 1) The slopes at the two ends of the member have equal magnitudes of the same sign. This follows from condition (A) above, 2) the sum of the amplitudes of the sine curves of deflections must add up to zero. This latter condition can be satisfied in a variety of ways. The buckled shape can consist of complete sine waves of alternately positive and negative signs but equal magnitudes, when the number of panels is even. The magnitudes of the amplitudes could be different but must add up to zero.

In an experimental verification of these results the panel which has the largest initial eccentricity will first bend and then buckle as the buckling load is approached. Other panels bend in such a way that they satisfy conditions (A) and (B) found above.

Results of the two loading experiments which are given in Part II of this paper, show that even with the unequal amplitudes of deflections in the first test and the unsymmetrical buckling phenomena which occurred in the second, conditions A and B were satisfied.

II. EXPERIMENTAL VERIFICATION OF THE BUCKLING LOAD

Two experiments were conducted to verify the foregoing derivation. The object was to verify both the buckling load and the buckling mode shape of the member.

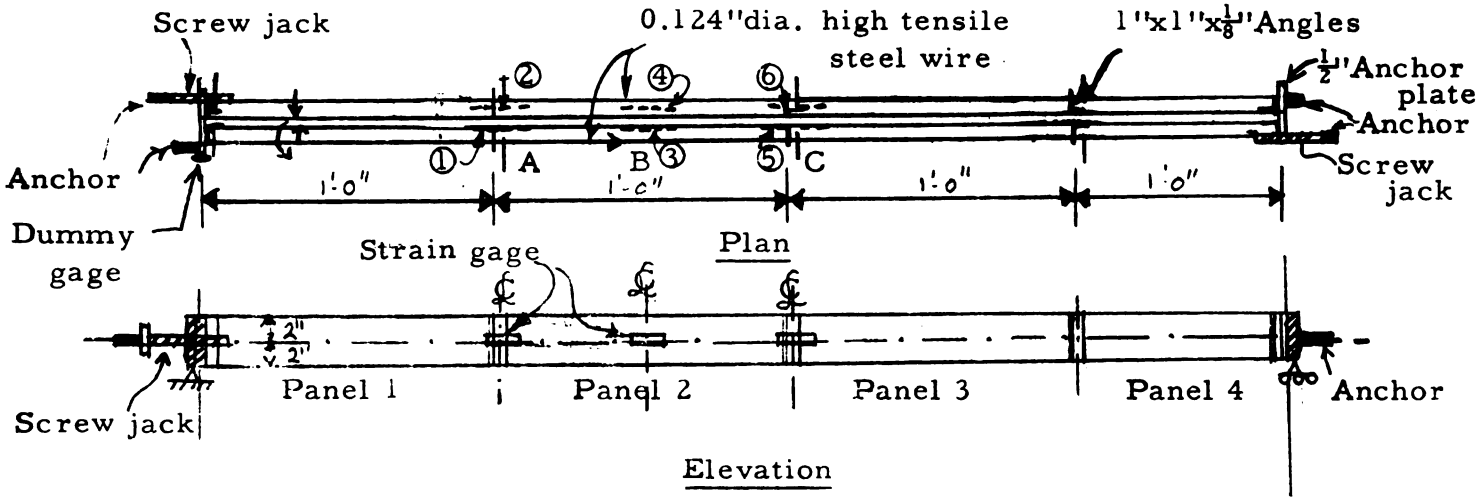

Figure 6 (not to scale)

1. Loading Experiment on an Aluminum Model

The test member was made of 3003-H-14 aluminum, which has a modulus of elasticity of 10×10^6 p.s.i. The member had a length of 4'0", a width of $\frac{1}{4}$" and was 4" deep. Spacers were made from 1" x 1" x $\frac{1}{8}$" aluminum angles and were fixed to the member by two $\frac{1}{4}$" diameter brass bolts. The spacing between the centers of outstanding angle legs was 1'0". High tensile steel wires, 0.124" in

diameter and with an ultimate strength between 270,000 and 300,000 p.s.i., were used as prestressing elements. One wire was placed on each side of the member at $\frac{1}{2}$" from the center line of the member. Strain gages were fixed at mid-depth on both the sides of the member at positions A, B and C shown in Figure 6. Gages at A and B were connected through a switching unit to the strain meter, with temperature compensating gages as dummy gages, fixed on the end anchor plates of the same material as the member. Gages at C were connected in the adjacent arms of the bridge, so that they recorded only the strains due to bending, the equal axial compressive stresses being balanced out. The center lines of all the gages at A and C, coincided with the center lines of the bolts connecting the angles to the member. It was proposed to ensure equal tensions on the two sides, by adjusting the jacks so that the gages at C gave no output. It was found that the bolt center lines on which the gages were fixed did not truly represent the points through which the resultant of the lateral components of the tensions on the two sides of the spacers passed, since the wire on the convex side of the curve pressed on to the spacer and that on the concave side pulled on the spacer. The compressive load exerted on the spacer was transmitted through the outstanding leg of the angle while the tensile load was transmitted to the member through the brass bolts. This caused a difference between the gage center line and the line on which the resultant of the lateral loads acted. As a result of this difference, when the bending moment at C was maintained zero, the beam was found to deflect on one side. This showed that the tensions on the two sides were unequal. It was decided to obtain symmetry and zero deflection at the center by adjusting the tensions on the two sides.

The first noticeable deflection occurred in panel 1, which was later followed by a similar deformation in panel 4. Gage readings were taken at frequent intervals to ensure that the strains did not attain very

large values. At the buckling load, however, the bend in panel 1 began to increase and all the strain gages showed continuous straining without corresponding increase in the tension in the wires. The tensions in the wires were immediately reduced until the strains were steady.

The strain meter readings for all the gages just before buckling took place, are tabulated below.

Gage No.	Strain (micro inches per inch)	Average	Station
1	-372	-321	A
2	-270		
3	-485	-332.5	B
4	-180		
5	110 diff. between 5 and 6		
6			

The average strain just before buckling was $\frac{321 + 332.5}{2}$ = 326.75 micro inches per inch.

σ = 326.75 x 10 = 3267.5 p.s.i.

Area of member = 4" x $\frac{1}{4}$" = 1 sq. in.

Buckling load = 3267.5 x 1 = 3267.5 lb.

Theoretical buckling load = $\frac{\pi^2 EI}{\ell^2} = \frac{\pi^2 \times 10 \times 10^6}{12 \times 12} \times \frac{4}{12} \times \frac{1}{64}$

for ℓ = 1'0".

= 3580 lb.

Percent difference = $\frac{313}{3580} \times 100$ = 8.75% between the experimental and the theoretical values

To find the deflection curve, dial gages were used at positions shown in Figure 7. Two readings were taken at each dial gage.

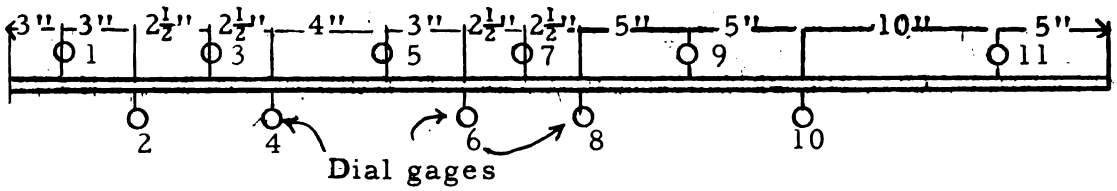

Figure 7 (not to scale)

One reading was taken in the maximum deflected state and the other when the tensions in the two wires were completely released. The pressures exerted by the dial gage spindles were sufficient to bend this slender member and to minimize this effect, the dial gages were fixed to the table on both sides of the member in a symmetrical manner. Because of the permanent deformation which occurred in panel 1, the deflection curve does not truly represent the ideal curve which is shown by dotted lines in Figure 8 on the following page. The buckling load, however, agrees well with the theoretical value.

2. Tests on Steel Model

The steel member had a section 3" x $\frac{1}{4}$" and a length of 4'6" between end anchors. Two intermediate spacers 1" wide and $\frac{1}{8}$" thick were welded to the member on both sides, thus dividing the member into three equal panels, each 1'6" long. Prestressing was accomplished by means of a high tensile steel wire placed on each side. Strain gages were fixed on both sides at positions A, B, C, D and E shown in Figure 9. Equal tensions on both sides were obtained by making the bending stresses at the point B equal to zero. Gages at the other stations recorded the strains at various positions in the span. They also served as a check on the total compressive load on the section.

Gage No.	Deflection (in).
1	+0.082
2	+0.127
3	+0.118
4	+0.120
5	+0.104
6	+0.062
7	+0.038
8	+0.038
9	-0.012
10	-0.023
11	-0.104

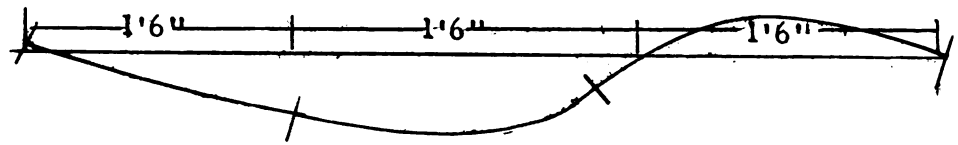

Figure 8(a). Steel model.

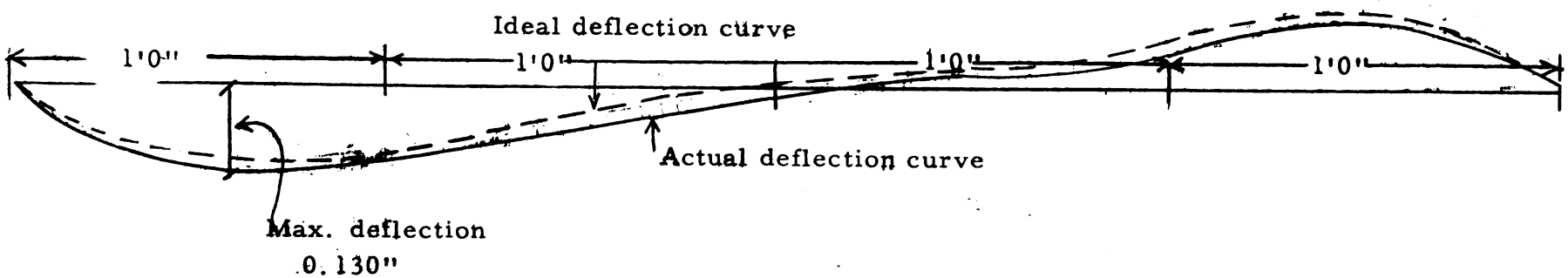

Figure 8

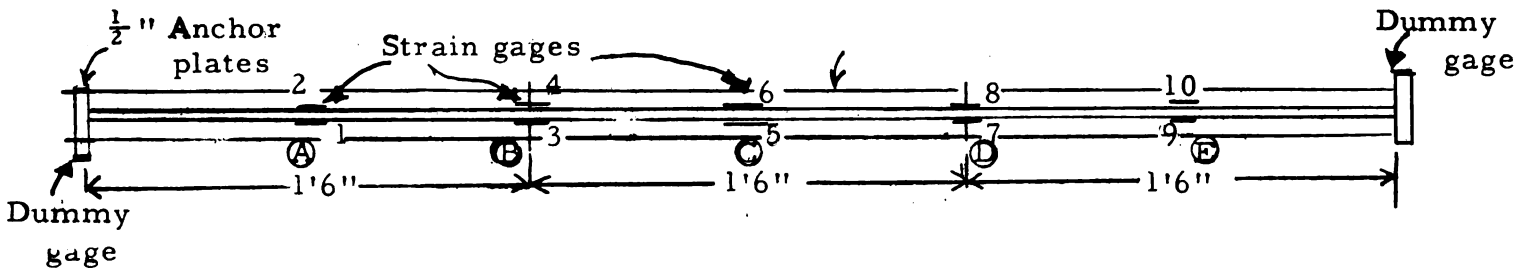

Figure 9 (not to scale)

The actual strains just before buckling were:

Gage No.	Strain (μ-inch/inch)	Average	Position
1	-158	-155	A
2	-152		
3	Difference maintained zero	—	B
4			
5	+290	-159	C
6	-608		
7	-150	-152.5	D
8	-155		
9	-595	-152.5	E
10	+290		

Average strain = 154.75 micro inches per inch

Corresponding stress = $154.75 \times 30 \times 10^6 = 4642$ lb per in^2.

Area = $3'' \times \frac{1}{4}'' = 0.75$ in^2.

Load = $4642 \times 0.75 = 3480$ lb.

Theoretical Load = $\frac{\pi^2 \times 30 \times 10^6}{18 \times 18} \times \frac{3}{12} \times \frac{1}{64} = 3560$ lb.

Deflections were not measured but the approximate deflected shape at buckling is sketched in Figure 8(a), page 16.

Conclusion

The results of the two experiments show that, 1) the buckling load is that obtained in the theoretical derivation, i.e., $P_{cr} = \frac{\pi^2 EI}{\ell^2}$, where ℓ is the length of the member between the adjacent spacers, 2) the slopes at the ends of the member are equal and of the same sign, and 3) the amplitudes of the sine curves of deflections are also equal but opposite in sign, so that their sum is equal to zero.

The buckling load found experimentally agreed well with the theoretical value. The buckled mode shapes were, however, not exactly what one would expect in a model having similar properties in all the panels. This discrepancy can be explained by the fact that, all the panels did not in fact have identical properties. Some of the panels may have had a greater built-in eccentricity than others. Bending of these panels may have dictated the mode shape of the whole member in its final buckled form.

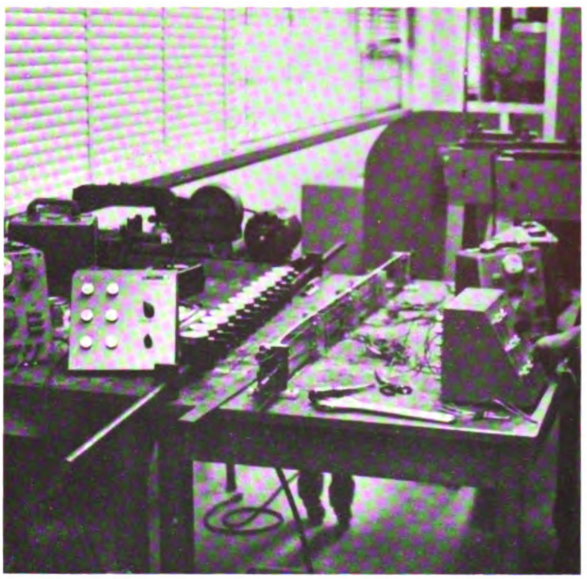

General Arrangement of the Apparatus for Experiment with the Aluminum Model.

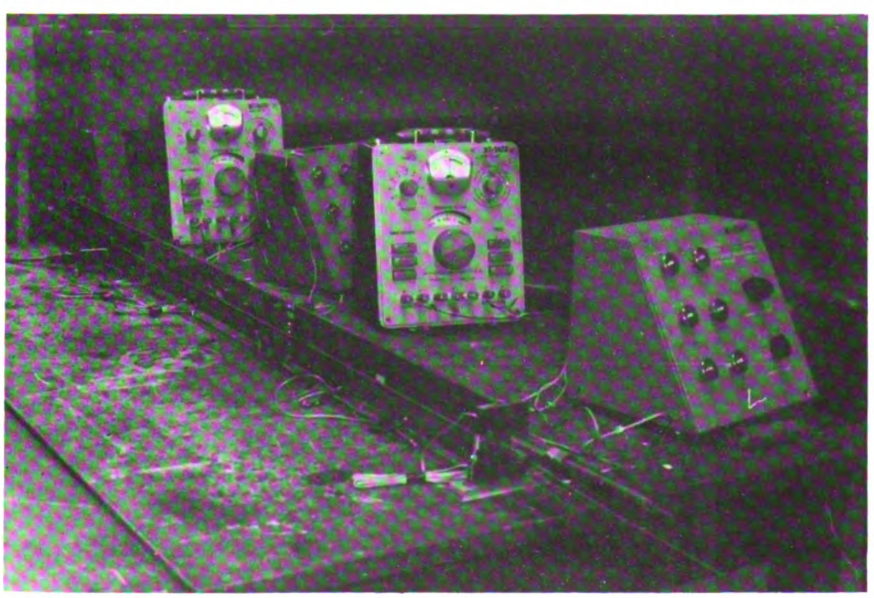

General Arrangement of the Apparatus for Experiment with the Steel Model.

III. APPLICATIONS

From the foregoing analysis and its experimental verification, it is apparent that the capacity of any structural member to sustain large compressive stresses, under prestress can be increased to any desired level, within the elastic range, by the use of spacers. With a sufficiently close spacing, the full working stress in compression can be induced in a member without causing instability.

Several applications to practical problems are possible. Simple tension carrying members can be effectively prestressed and their load resisting capacity increased. An extension of this idea to indeterminate trusses will be more economical since prestressing tension carrying members will induce stresses of opposite kind in other members as well. However, with the availability of high strength steels in the form of the usual structural sections, such applications lose their significance. As in the prestressed concrete construction prestressing can be effectively utilized in steel construction as well. Steel can resist both the tensile and compressive stresses equally well and hence there is no limitation to the maximum eccentricity. Thus with a smaller prestressing force, large moments can be induced in the girder. Full advantage of the prestressing technique cannot, however, be realized in steel construction because of the reasons mentioned below:

With an eccentric prestressing force, the tension flange can be prestressed to the full allowable stress in compression. But on account of the presence of the direct compression, uniform over the whole section, which has to be superimposed on the bending stresses due to the eccentricity of the prestressing force, the maximum tensile stress in the compression flange is much lower than the permissible

tensile stress. Under the action of external loads, then, the controlling design consideration is the compression in the compression flange, while the tension flange remains understressed. This is particularly true in the case of symmetrical sections such as rolled I beams. With an unsymmetrical section having a larger tension flange, it may become possible to have a greater range of stress in the compression flange between the loaded and the unloaded states of the beam. With a small compression flange, however, the problem of its buckling under full working load, then is of primary concern.

This drawback is automatically overcome in the composite construction in steel and concrete. The addition of a large area on the top flange, by way of the concrete slab connected to the steel girder by shear connectors, increases the modulus of the composite section with respect to the top, compression flange. The stress variation due to the superimposed loading is, therefore, much greater in the tension flange than it is in the compression flange. Full working stresses under maximum load, can then be simultaneously reached in both the flanges, by suitably proportioning the section.

In the following few paragraphs, the various advantages possible in prestressed composite construction are enumerated.

Many of these observations are with particular reference to large span bridge girders, in which use of unsymmetrical sections is possible. No attempt is made to present detailed design calculations and anyone interested is referred to serial nos. 5 and 6 of the bibliography.

Figures 10(a) to 10(d)(on the following page) show diagramatically the various loading stages, section properties and the stress variation across the section at each of the loading stage. Different moduli of elasticity for concrete under permanent and nonpermanent loads have been assumed. These assumptions are based on those made in

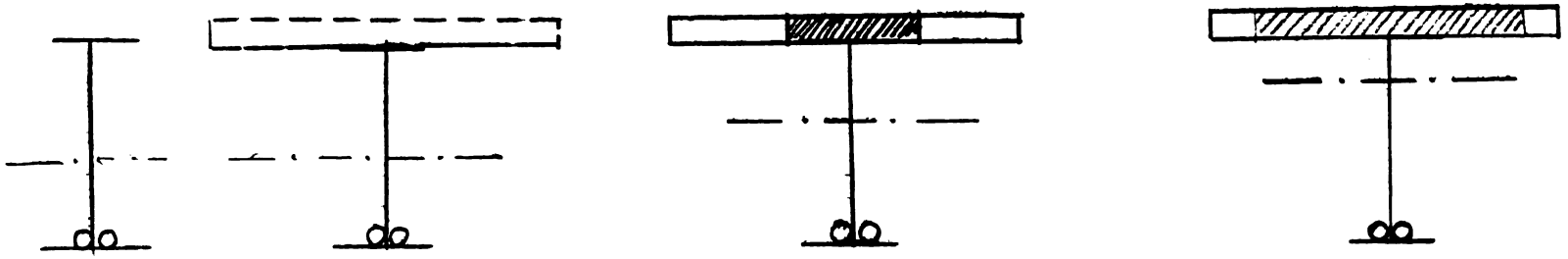

1. Prestressed girder (a)

2. Girder with slab d. 1. (b)

3. Girder under composite d. 1. (c)

4. Girder under live load (d)

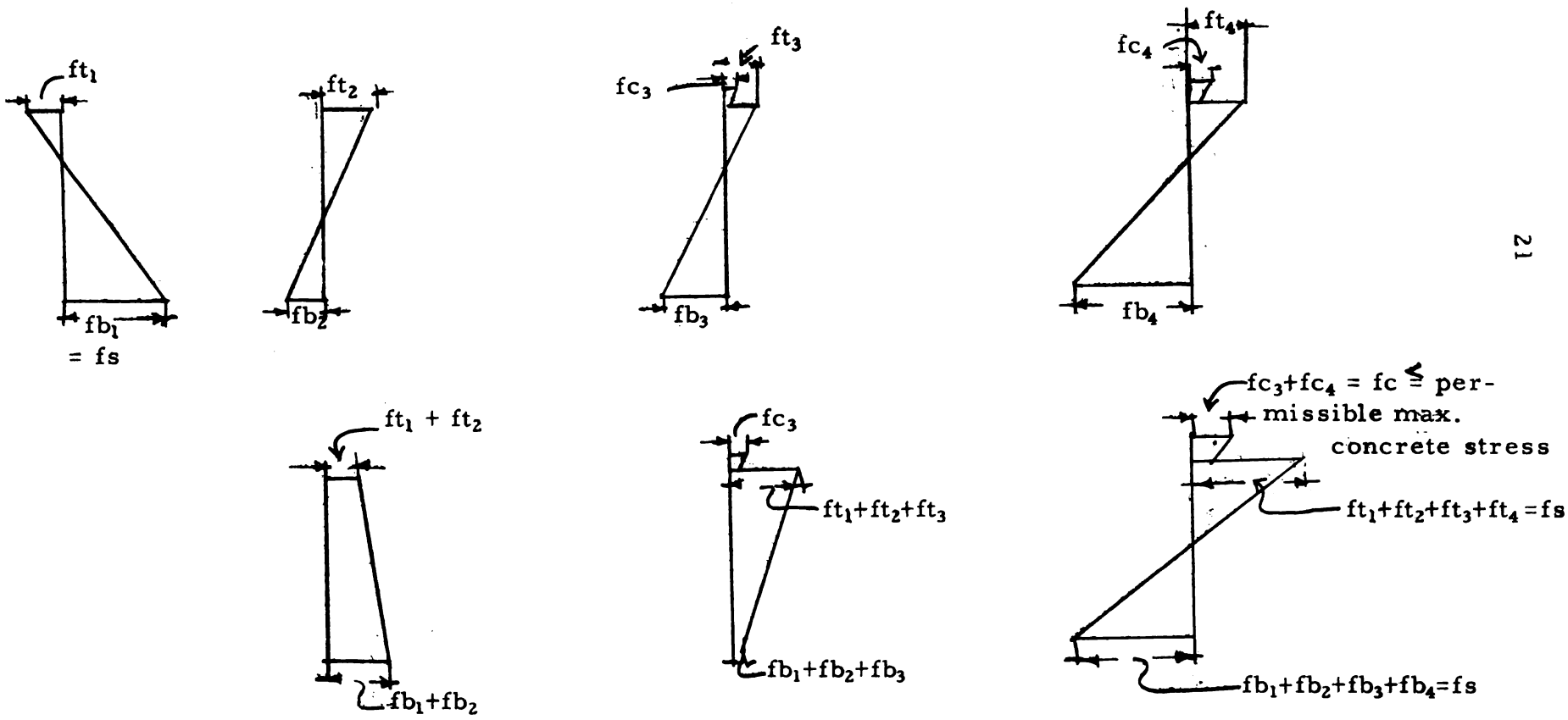

Figure 10

"Composite Construction in Steel and Concrete" (reference 1 in the Bibliography). The same textbook may be referred to for other particulars such as choice of trial section, calculation of section properties of composite and noncomposite sections and stresses.

The many advantages resulting from using prestressing technique are enumerated below. Some of these observations are based on the stress variations at the different states of loading, sketched in Figures 10(a) to 10(d), to which reference is made.

1. For the bottom flange, the change in stress is from $-f_s$ to $+f_s$ where f_s is the maximum permissible stress in steel. The effective stress utilization is therefore twice that for normal structural steel construction.

2. The top flange, under prestress, carries a small tensile stress. The working stress range in this region though not as large as in the case of the bottom flange is still significant.

3. The top flange is adequately supported along its entire length by its rigid connection to the concrete slab by shear connectors. The compressive stress can therefore be as high as the full allowable stress in steel.

4. The utilization of the full working stress in both the flanges is made possible by the addition of concrete slab. Whereas, the stress in the bottom flange varies from $-f_s$ to $+f_s$, the variation in the top flange is not so large. However, the addition of further area on the top flange by way of the concrete slab, while increasing the moment of inertia of the section considerably, shifts the neutral axis of the composite section very near to the top flange. This results in a large increase in the modulus of section with respect to the top flange. The resulting stresses on account of the composite dead load bending moment and the composite live load bending moments in the top flange are much lower than those in the bottom flange. A judicious selection of the

section therefore makes it possible for the full working stress to be reached simultaneously in both the flanges.

5. A major portion of the compressive strength of the slab in the longitudinal direction is utilized in resisting moments due to superimposed loading. This results in further economy.

6. Shear resistance of the girder is increased. The vertical components of the prestressing forces offer part of the resistance to external shears, thus relieving the girder web of this part of the total shear.

7. Loss in prestress due to creep is much less significant than in prestressed concrete construction.

8. Gain in prestress due to deformation of the girder under load is significantly larger than in prestressed concrete. This is so because of the proportionately larger area of the prestressing steel. This large gain offers a greater resistance to moments.

9. The construction being light, the dead load moments are very much smaller.

10. Girders can be fabricated and prestressed in the shops and erected directly on the superstructure. The erection may require little or no shoring.

11. Slab formwork can be directly supported on the steel girder. This saves considerable shoring needed for supporting the slab formwork.

The design of prestressed composite structures is much more complex than similar unprestressed structures or non-composite structures. This is so because the design depends on several parameters. Proportions of dead load, composite dead load and live load moments will dictate the initial choice of trial section. For example, if the proportion of non-composite dead load moment is high, the girder section will have to be comparatively heavy and unsymmetrical,

with a larger tension flange. The relative magnitudes of steel and concrete areas will decide the position of the neutral axis for the composite section. Since the slab thickness is decided on strength requirements in a direction transverse to the length of the beam, any variation required in the slab thickness will necessitate changes in girder spacing. The prestressing cable profile will largely be decided on the type of loading. Shear resistance offered by the prestressing cables will in turn depend on the cable profile. The external shear and part resisted by the prestressing cables decide the web area required. On the proportions of web area to the total steel area and to the top and bottom flanges depend the properties of the section.

All these interdependent factors make the design of composite, prestressed structures a very complex problem. With any improvement in the technique, such complexities are inevitable.

The prestressing technique, using spacers, can be advantageously used for prestressing thin plates and shells. While the more complicated two and three dimensional problems are outside the scope of this paper, the principle can be illustrated for a line structure such as a plate simply supported on two opposite edges.

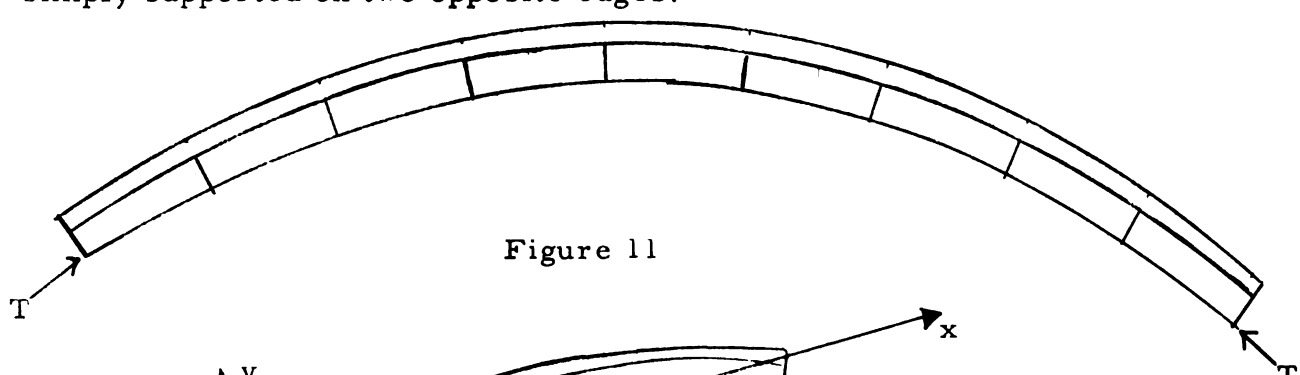

Figure 11

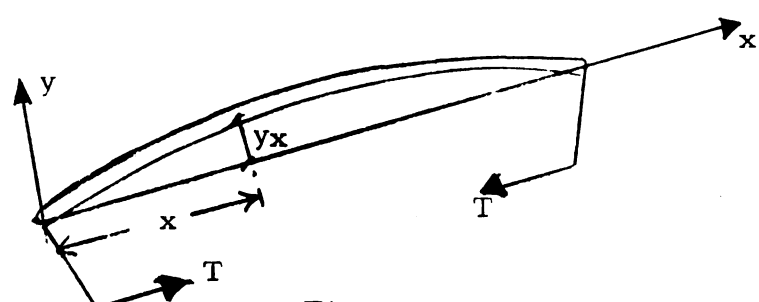

Figure 11(a)

Figure 11 shows such a plate under the action of prestressing force, applied on one side of the plate, by means of high tensile steel wire, which passes through a number of spacers. The spacers maintain the distance 'd' between the wire and the center line of the plate at those points where the wire passes through the spacers. Figure 11(a) shows one panel of the plate between any two adjacent spacers. Each such panel is acted upon by two collinear forces T acting at a fixed eccentricity d at the two ends.

Let y_x be the deflection of any point in the plate panel. The 'x' axis is the chord joining the ends of the panel.

The bending moment at this point is

$$- EIy''_x = T (d + y_x) \quad \ldots\ldots\ldots \text{(i)}$$

or

$$y''_x + \frac{T}{EI} y_x + \frac{T}{EI} d = 0 \quad \ldots\ldots \text{(ii)}$$

Letting $\frac{T}{EI} = p^2$, solution of this equation is,

$$y_x = C_1 \cos px + C_2 \sin px - d \quad -- \quad \text{(I)}$$

For $x = 0$

$$0 = C_1 - d \text{ from which } C_1 = d \quad \ldots\ldots \text{(iii)}$$

and for $x = \ell$

$$0 = C_1 \cos p\ell + C_2 \sin p\ell - d \text{ from which}$$

$$C_2 = d \frac{(1 - \cos p\ell)}{\sin p\ell} \quad \ldots\ldots\ldots \text{(iv)}$$

$$y_x = d \left(\cos px - 1 + \frac{1 - \cos p\ell}{\sin p\ell} \sin px\right) \quad \ldots\ldots \text{(II)}$$

y_x becomes infinitely large for $p\ell = n\pi$ where n is odd and in particular for $p\ell = \pi$

The critical load is therefore $T = \frac{\pi^2 EI}{\ell^2}$ as before, where EI refer to the properties of the plate.

The spacing can always be so adjusted, that the design consideration under the prestressing load, is the maximum compressive stress due to bending and direct force, and not instability. The distance d can be suitably adjusted for the kind of plate being prestressed. Thus for a simply supported plate, the distance d would be the minimum practicable at the ends increasing to some predetermined value at the centre, linearly or parabolically, depending on loading. The significantly large gain in prestress, as the plate deforms under loading, further increases resistance to moment. For a plate material with a modulus of elasticity considerably lower than that of steel such a gain can be really significant.

The following simple example illustrates the increase in load carrying capacity of a simply supported plate. The Engineer's Theory of Bending is used and although it is not strictly accurate because of large deflections involved, it can be a rough guide for comparison.

Consider an aluminum plate, $\frac{1}{4}$" thick and 12" wide, simply supported at the ends of a span of 3'0".

The plate is prestressed by high tensile steel wire 0.03 sq. in. in area and placed through spacers, at an eccentricity of $\frac{1}{8}$" at the ends increasing linearly to $\frac{3}{8}$" at the centre of the span, at the bottom of the plate.

Let T be the initial tension.

Max. stress at the bottom fibre

$$= \frac{T}{12 \times \frac{1}{4}} + T \times \frac{3}{8} \times \frac{16 \times 6}{12} = \frac{T}{3} + 3T = 3.33T \text{ lb. per sq. in.}$$

If the maximum permissible stress in the plate is 10,000 p.s.i.

3.33 T = 10,000 and T = 3,000 lb.

Let W be the maximum concentrated central load on the plate and let δT be the increase in prestressing force in the wires.

Change in Bending moment at any section = $\frac{W}{2} \cdot x - (\delta T)(\frac{1}{8} + \frac{x}{18} \cdot \frac{1}{4})$

Rotation of the elementary length dx =

$$\frac{1}{EI} \left\{ \frac{W}{2} x - (\delta T) \left(\frac{1}{8} + \frac{x}{72} \right) \right\} dx.$$

Assuming $E = 10 \times 10^6$ p.s.i.

$$\delta\theta = \frac{64}{10^7 x}\left\{\frac{W}{2}x - (\delta T)\left(\frac{1}{8} + \frac{x}{72}\right)\right\} dx.$$

Change in length of a small element dx of the wire =

$$\frac{64}{10^7}\left\{\frac{W}{2}\cdot x - (\delta T)\left(\frac{1}{8} + \frac{x}{72}\right)\right\}\left(\frac{1}{8} + \frac{x}{72}\right) dx$$

Total change in length of the wire

$$= 2 \times \frac{64}{10^7}\int_0^{18}\left\{\frac{W}{2}x - (\delta T)\left(\frac{1}{8} + \frac{x}{72}\right)\right\}\left(\frac{1}{8} + \frac{x}{72}\right)dx.$$

$$= \frac{128}{10^7}\left\{23.62\,W - 1.22\,\delta T\right\}$$

Change in the tension in the wires

$$= \frac{128}{10^7}\,(23.62W - 1.22\,\delta T) \times 0.03 \times \frac{3 \times 10^7}{36}$$

$$= 7.55\,W - 0.39\,\delta T = \delta T$$

$$\therefore\ \delta T = \frac{7.55W}{1.39} = 5.43\,W.$$

Max. stress at the top fibre in the loaded state

$$= \left\{W.\frac{36}{4} - (3000 + 5.43\,W)\cdot\frac{3}{8}\right\} \times \frac{16 \times 6}{12} + \frac{3000 + 5.43\,W}{3}$$

$$= 57.52\,W - 8000 = 10,000 \text{ p.s.i.}$$

$$\therefore\ W = \frac{18,000}{57.52} = \underline{315}\text{ lb.}$$

For an unprestressed plate if W' is the max. central concentrated load,

$$\left(W'.\frac{36}{4}\right)\frac{16x6}{12} = 10,000$$

$$\therefore\ W' = \frac{10,000}{72} = \underline{139}\text{ lb.}$$

Additional load capacity $= \frac{315}{139} \times 100 = 226\%$.

Total load in the wire = 3000 + 5.43 x 315 = 4710 lb.

Stress in the wire = $\frac{4710}{0.03}$ = 157,000 p.s.i.

Max. stress at the end supports = 1.33 x 4710 = 6260 p.s.i.

Conclusion

The pre-stressing technique, using spacers, opens up immense possibilities for designing light, economical structures at a fraction of their present costs. While only very simple structures have been discussed in this paper, the idea can obviously be extended to more complex structures such as plates and shells. Further research in this field, it is hoped, will pave the way for very light and stiff structures to meet our future needs.

BIBLIOGRAPHY

1. Composite Construction in Steel and Concrete by Viest, Fountain and Singleton, McGraw Hill Book Co., 1958.

2. Theory of Elastic Stability, S. Timoshenko and J. Gere, McGraw Hill Book Co., 2nd Ed., 1961.

3. Prestressed Steel Structures, G. Magnel, The Structural Engineer, Vol. 28, No. 11, Nov. 1950.

4. Prestressed Truss Beams, R. L. Barnell, Transactions, ASCE, Vol. 124, 1959.

5. Design of Prestressed Composite Steel Structures, R. Sziland, Proceedings, ASCE, Vol. 85, No. St.9, Nov. 1959.

6. Behaviour of Prestressed Composite Steel Beams, Peter G. Hoodley, Journal of Structural Division, Proceedings ASCE, June 1963.